Evidence of tendon microtears due to cyclical loading in an in vivo tendinopathy model

Leena H. Nakama [a], Karen B. King [a,b], Sven Abrahamsson [c], David M. Rempel [a,b,*]

[a] Joint Graduate Group in Bioengineering, University of California, Berkeley and San Francisco, CA, USA
[b] Department of Medicine, University of California, San Francisco, CA, USA
[c] Department of Hand Surgery, Malmo University Hospital, Malmo, Sweden, CA, USA

Abstract

Tendon injuries at the epicondyle can occur in athletes and workers whose job functions involve repetitive, high force hand activities, but the early pathophysiologic changes of tendon are not well known. The purpose of this study was to evaluate early tendon structural changes, specifically the formation of microtears, caused by cyclical loading. The Flexor Digitorum Profundus (FDP) muscle of nine New Zealand White rabbits was stimulated to contract repetitively for 80 h of cumulative loading over 14 weeks. The contralateral limb served as a control. The tendon at the medial epicondyle insertion site was harvested, sectioned, and stained. Microtears were quantified, using image analysis software, in four regions of the tendon, two regions along the enthesis and two distal to the enthesis. The tear density (loaded: 1329 ± 546 tears/mm^2; unloaded: 932 ± 474 tears/mm^2) and mean tear size (loaded: 18.3 ± 6.1 µm^2; unloaded: 14.0 ± 4.8 µm^2) were significantly greater in the loaded limb ($p < 0.0001$) across all regions compared to the unloaded contralateral limb. These early microstructural changes in a repetitively loaded tendon may initiate a degenerative process that leads to tendinosis.
© 2005 Orthopaedic Research Society. Published by Elsevier Ltd. All rights reserved.

Keywords: Microtears; Epicondylitis; Tendinopathy; Overuse; Tendon

Introduction

Tendon injuries due to overuse are a common problem in athletes and workers and account for 30–50% of all sports-related injuries [11,12] and almost half of occupational illnesses in the United States [29]. Epicondylitis, a tendinopathy at the elbow, is a common disorder in adults; the incidence in general practice is approximately 4–7 per 1000 patients per year with an annual incidence of 1–3% in the general population [1,7]. Although epicondylitis is related to forceful and repetitive hand activities, little is known about the early mechanisms of injury that ultimately lead to tendinopathy. Elucidating the early structural, cellular, and molecular changes in the tendons exposed to cyclical loading may ultimately improve prevention and treatment options.

Lateral epicondylitis is an injury of the common extensor tendon at the lateral epicondyle while medial epicondylitis is an injury to the common flexor tendon at the medial epicondyle. Epicondylitis presents as localized pain, tenderness, and occasionally swelling [33]. Biopsies of the tendon and surrounding scar tissue in patients with epicondylitis reveal fibrovascular and cellular proliferation, intratendinous calcification and cartilage formation, loss of parallel tendon fibers, fibrofatty degeneration, and partial tendon rupture [6,13,20–22, 25]. The absence of inflammatory cells has led some authors to propose the term tendinosis instead of tendonitis [13,15,23].

* Corresponding author. Address: University of California, 1301 South 46th Street. Building 163, Richmond, CA 94804, USA. Tel.: +510 231 5721; fax: +510 231 5729.
E-mail address: drempel@itsa.ucsf.edu (D.M. Rempel).

Large tears (~ 1 cm^2) have been observed in tendons of humans with tendinosis using high-resolution ultrasound [10,14], MR imaging [8,25,34], and 3D volume-rendered images from multi-detector computer tomography (MDCT) [19]. However, no animal or human studies have investigated the tendon for smaller structural defects or microtears, on the scale of 1–500 μm^2, that may occur early following cyclical loading.

The purpose of this study was to evaluate microstructural changes, specifically microtear formation in the Flexor Digitorum Profundus (FDP) tendon at the medial epicondyle following cyclical finger loading using a rabbit model. Rabbits were used because the FDP muscle could be isolated for electrical stimulation using small percutaneous needles. In spite of some anatomical differences, the general structure of the tendon insertion site at the epicondyle and the composition and biology of tendon healing in rabbits are similar to that in humans [3,4,9,16,26].

Methods

Animal model

Nine female, young adult, New Zealand White rabbits weighing 3.49 kg (± 0.30) were used. Under general anesthesia, the FDP muscle of one forelimb was electrically stimulated to contract repetitively for 2 h per day, 3 days a week, for 80 cumulative hours of loading. The contralateral limb, although supported in the same posture as the loaded limb during loading, did not receive a stimulus and served as the control. This study was approved by the University of California, Berkeley's Committee on Animal Research.

After inducing anesthesia with isoflurane, the rabbit was placed in a supine position with the forearms loosely secured to supports (Fig. 1). A muscle stimulation needle (33G) was inserted subcutaneously in the middle of both forearms so that the needle barrel was in contact with the surface of the FDP muscle, and the needle tip was pushed back through the skin. A lightweight, brass glove was slipped over digit 3 of the stimulated limb and connected to a load cell by a wire to mea-

sure the flexion force of the digit due to FDP contraction. The muscle was stimulated (S48 and SIU5, Grass Instruments) with 1 Hz pulse trains with train durations of 200 ms, pulse widths of 2 ms, and pulse rates of 100 pulses/s. The stimulation voltage was adjusted (6–12 V) to maintain a mean peak fingertip force of 0.42 N (15% of peak tetanic force). The resultant load was selected to be within the physiologic range of the muscle and the number of repetitions is within that experienced by workers who perform repeated tasks [18]. The control limb was not electrically stimulated.

After 2 h of cyclical loading, the stimulation electrodes and finger glove were removed, the anesthesia was discontinued, and the rabbit was returned to its cage. This process was repeated 3 days per week for a total of 80 h of stimulation. Weekly examinations of the paw, forearm, and elbow revealed no tenderness, limping, nodules, swelling, limitation in range of motion, reduction in gross claw flexion strength, or skin breaks.

Tissue and histological preparation

After 80 h of cumulative loading, the animals were weighed (3.89 ± 0.19 kg) and euthanized. Evaluation of the subcutaneous area at the stimulation needle insertion site revealed minimal scar tissue localized within 5 mm of the needle insertion site; the scar tissue did not extend to the FDP tendon. Both medial epicondyles were dissected free with the FDP tendon and muscle attached, fixed in 10% formalin for 24 h, decalcified in EDTA for three weeks, paraffin embedded, and sectioned 7 μm longitudinally.

Nine serial sections from the center of the tendon block were deparaffinized, rehydrated, stained (Iron Hematoxlin, Safranin-O and Fast Green), dehydrated, and cover slipped. Safranin O and Fast Green staining was used as a contrast agent to distinguish tears (non-staining regions) from intact tendon tissue. Histological preparation and staining were completed at the same time for tissue from both limbs. Histologists were blinded to specimen loading status.

Image acquisition and analysis

Four regions of interest (ROI) (Fig. 2) were digitally photographed under 200× magnification using Axiovision software v3.1 and an Axioskop2 microscope with an Axiocam digital camera (Carl Zeiss, Germany). Prior to image acquisition, the camera was white balanced to ensure a uniform background color. The microscope's light intensity was maintained at a constant level to ensure the background mean gray values of the images were similar throughout the image acquisition process.

The images were cropped to contain only the ROI. The boundaries of all the non-staining areas in the tendon (e.g., tears) were identified using custom software (IMAQ, National Instruments Vision Builder
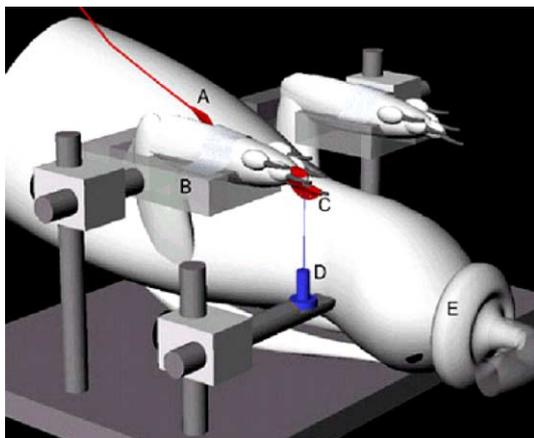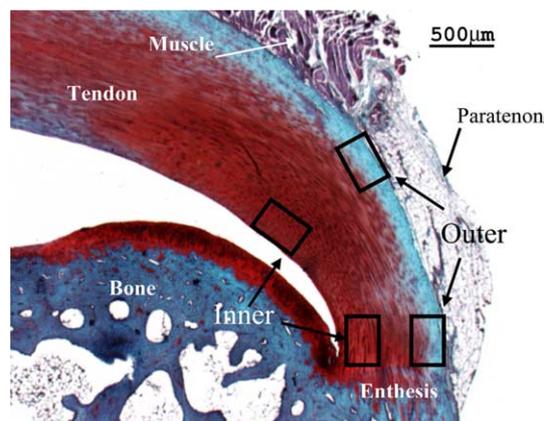

Fig. 1. Cartoon of the loading apparatus with rabbit in a supine position with head to the right and forearms supported: (A) stimulation needle, (B) forearm support, (C) third digit with metal glove, (D) load cell and (E) anesthesia mask.

Fig. 2. Epicondyle with bone, tendon, paratenon, and muscle. Four regions of interest are highlighted, two along the enthesis, and two 1500 μm distal to the enthesis. The regions of interest are 200 μm by 400 μm.
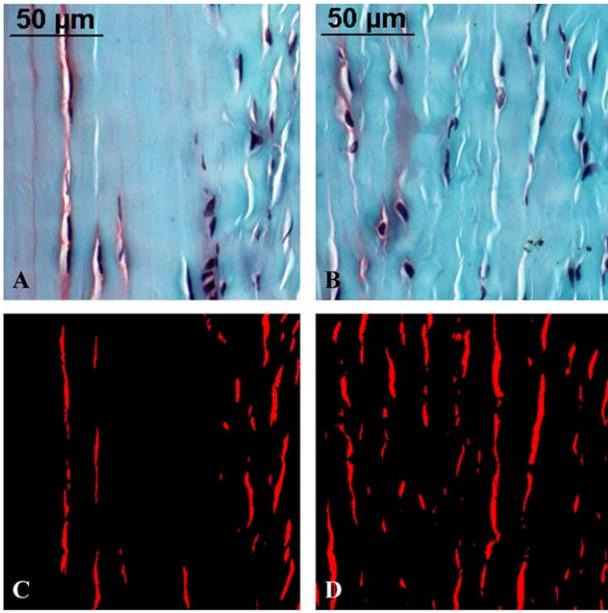
Fig. 3. Unloaded (A) and loaded (B) tendon stained with Iron Hemotoxilin, Safranin O and Fast green. Thresholded images in same unloaded (C) and loaded (D) tendon identify microtears as red regions.

6) to threshold gray values (Fig. 3). Thresholded values were selected based on mean gray values of tears present in each ROI, and thresholded images were compared to the original ROI image to ensure all tears were captured in the thresholding process. All tears of sizes 3–300 μm^2 were quantified; smaller or larger tears could be considered artifacts and were not included in the analysis.

Summary measures of all of the tears for each ROI were calculated (tear area as a percent of tendon area, tear density, and mean tear size). The distribution of tear sizes were determined by sorting tears from 3–10 μm^2 in size into intervals of 1 μm^2, 3–100 μm^2 in size into intervals of 10 μm^2, and 3–300 μm^2 in size into intervals of 100 μm^2. Image acquisition and analysis were performed blinded to specimen loading status.

Statistical analysis

A mixed model repeated measures ANOVA was used to analyze differences in tear measures by region (inner enthesis, outer enthesis, inner distal, or outer distal) and by limb loading status (loaded or unloaded). Post hoc analysis was performed using the Tukey method for multiple comparisons. The distributions of tears by tear size were transformed into normal distributions using a log transformation preceded by the addition of the smallest value to each data point to avoid taking the logarithm of a zero, then the transformed tear densities were compared between loaded and unloaded limbs with the paired *t*-test with $\alpha \leqslant 0.01$ to adjust for multiple comparisons.

Results

Across the four ROIs, the mean tear area as a percent of total tendon area ranged from 0.8% to 4.5% in the loaded tendon compared to 0.4–3.1% in the unloaded tendon (Fig. 4A). The limb by region interaction term in the ANOVA was significant ($p < 0.007$). Using the Tukey follow-up test, significant differences between regions and exposure status were found. In Fig. 4, the
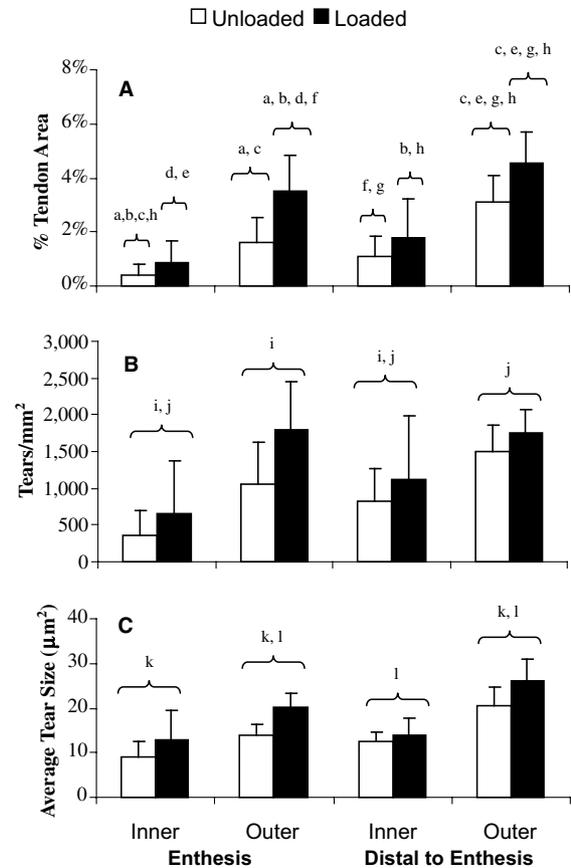

Fig. 4. The tear area as a percent of tendon area (A) has a significant limb by region interaction term, whereas the interaction term for the tear density (B) and average tear size (C) were not significant. These endpoints were significantly higher in the loaded limbs compared to unloaded limbs regardless of region. Regions marked with the same lower case letter are significantly different, based on the Tukey follow-up test. Columns are mean ± SD.

same letter marks columns that are significantly different. The loaded limb had a higher percent of tear area than the unloaded limb in the outer regions of the tendon, both at the enthesis ($p < 0.0001$) and distal to the enthesis ($p = 0.001$). In contrast to this finding, the inner regions of the tendon, at the enthesis ($p = 0.85$) and distal to the enthesis ($p = 0.40$), did not have significantly larger tear area percents in the loaded limbs when compared to the unloaded limbs.

Mean tear density ranged from 650 to 1788 tears/mm^2 in the loaded tendon and 358–1491 tears/mm^2 in the unloaded tendon across the four regions of interest (Fig. 4B). The limb by region interaction term was not significant ($p = 0.22$). Loaded limbs had significantly greater microtear densities than the unloaded limbs ($p < 0.0001$), regardless of region. Based on the Tukey follow-up tests, there were regional variations; the inner enthesis region had a significantly lower microtear density than the other three regions ($p < 0.003$). The inner distal region had a significantly lower microtear density
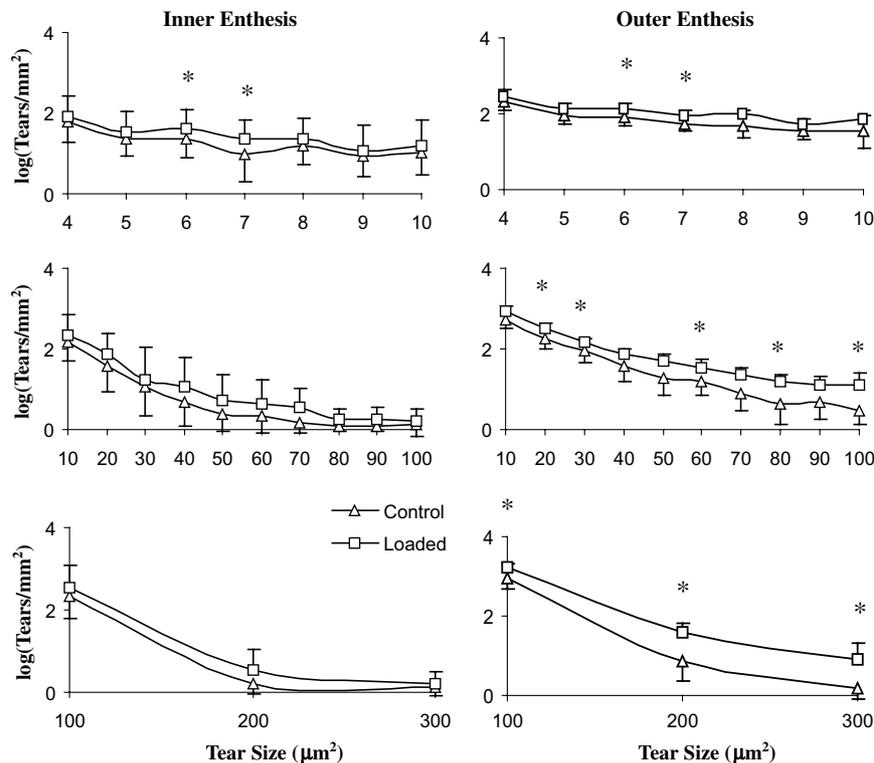
Fig. 5. The log of the distribution of microtears by tear size is shown (±SD) for the inner and outer regions of the tendon along the enthesis (*n* = 9). Significant differences between unloaded and loaded limbs for each microtear size are indicated with an * (paired *t*-test, *p* < 0.01).

than both the outer enthesis (*p* = 0.003) and the outer distal region (*p* < 0.0001).

The mean tear sizes ranged from 13 to 26 μm^2 in the loaded tendon and from 9 to 21 μm^2 in the unloaded tendon, across the four regions of interest (Fig. 4C). The limb by region interaction term was not significant (*p* = 0.27); the loaded limbs had significantly larger tears (*p* < 0.0001), regardless of region. There were also significant regional differences based on the Tukey follow-up tests. The outer region distal to the enthesis had significantly larger mean tear sizes than the other regions (*p* < 0.02). The outer enthesis had significantly larger tears than the inner enthesis (*p* = 0.0001) and the inner distal region (*p* = 0.019).

The distribution of tears by size varied by region and loading status. Across all tear sizes the tear density was higher in the loaded tendon than the unloaded tendon (Figs. 5 and 6). At the enthesis, significant differences were observed primarily in the outer region, almost evenly distributed across tear sizes. Distal to the enthesis, significant differences were observed in the outer region, primarily in the larger tear sizes.

Discussion

This is the first study to examine tendons for microtear (3–300 μm^2) formation in response to cyclical load-

ing in an in vivo animal model. All three measures of tear (tear area as a percent of tendon area, tear density, and mean tear size) were significantly greater in the cyclically loaded tendon compared to the unloaded tendon. In addition, there were variations in tear measures by region. The outer regions of the tendon, both at the enthesis and distal to the enthesis, had a greater tear density and a larger mean tear size than the inner regions. The observed regional differences in tear distribution may be due to differences in stress distributions in the tendon. As the FDP tendon is loaded, the region adjacent to bone (inner enthesis) experiences compression as well as tension resulting in fibrocartilage formation [16,31]. Fibrocartilage has different mechanical and biological properties that allow it to absorb compressive stresses [30,32]. Therefore, the inner and outer enthesis are structurally different and may have different modes of failure under repetitive loads.

Wakabayashi et al. [32] used finite element analysis to estimate the stress distribution in the supraspinatus tendon, which attaches to bone in a similar arrangement as the FDP attaches to the medial epicondyle. The stresses in the tendon are not uniformly distributed throughout a loaded tendon. This differential stress distribution is likely to be present in the FDP tendon and may explain the increase in tear density in the outer enthesis and mean tear size in the different regions of the FDP rabbit tendon in our animal model.
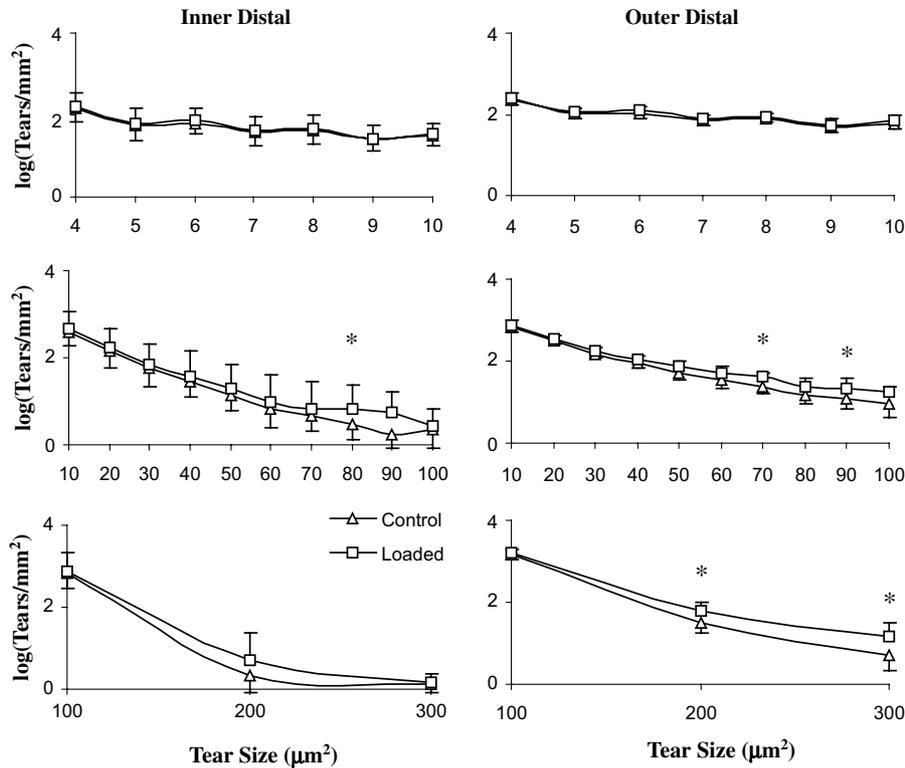
Fig. 6. The log of the distribution of microtears by size is shown (±SD) for the inner and outer parts of the tendon distal to the enthesis ($n = 9$). Significant differences between unloaded and loaded limbs for each microtear size are indicated with an * (paired *t*-test, $p < 0.01$).

Previous in vivo cyclical tendon loading studies offer varying findings. Backman et al. [4] used rabbits in a chronic Achilles tendinosis model ($N = 13$, 30–36 h of cumulative loading) and found changes in the paratenon and tendon, most notably tendon fibrillation and an increased number of inflammatory cells and blood vessels after repetitive eccentric exercise. The semiquantitative results showed changes to the entire tendon and paratenon but did not focus on specific areas within the tendon, such as near the tendon–bone junction or the tendon–muscle interface. Archambault et al. [3] also used a rabbit to model Achilles tendinosis ($N = 4$, 66 h of cumulative loading); no changes in degeneration or density of inflammatory cells were found, but some suggestion of an increase in mRNA expression of collagen III and IL-1β and decrease in expression of IGF-II were noted. Backman et al. used a loading frequency of 2.5 Hz, which was twice that used in Archambault's study. The loading frequency was decreased in the Archambault study because it was considered a slow hopping rate for rabbits and within physiological limits. Mean tendon force was 26 N in the Archambault study; tendon load data was not available for the Backman study. These studies did not evaluate the tendon for microtears.

Other investigators studying the effect of overuse injuries in human biopsy specimens and animal loading models have reported a disruption in collagen fiber organization, tendon fibrillation, and tendon thickening [4,5,17,24,27]. These structural effects may alter the tissue's gross mechanical properties. Soslowsky et al. [24] found a decreased maximum tensile load on loaded tendons after 20 h of cumulative loading in rats undergoing a repetitive exercise protocol that consisted of treadmill running. At longer loading periods, they reported larger cross-sectional tendon areas, decreased moduli, smaller allowable maximum stresses, increased cellularity, collagen disorganization, and changes in cell morphology in a loaded tendon compared to non-exercised cage control rats. Barbe et al. [5] reported tendon fibrillation and an infiltration of macrophages in their rat tendinosis model after 18 h of cumulative repetitive loading that involved rats reaching for food. Although the animals had a preferential limb to use for the task, they did not compare these results to the non-loaded limbs of the same animals, but rather to cage controls. Macrophages are known to release pro-inflammatory cytokines and metalloproteinases following repetitive loading injury of tendon fibroblasts and these may induce the degradation of the collagen matrix [2,28]. Matrix degradation may lead to mechanical instability and the formation of microtears. Some weaknesses of the aforementioned studies include a lack of characterization and control of the biomechanical loads.

Limitations of this study should be considered. First, the ROI's selected did not cover the whole tendon and missed, for example, the important tendon–muscle junction region. Second, the tissue preparation included formalin fixation and paraffin-embedding, which required heat treatment and dehydration of the tissue, which could disrupt tissue architecture and cause tendon fibers to separate. Therefore, measures for microtears in both limbs may have been increased by the histological preparation. However, the tissues were prepared and analyzed simultaneously, the histology technicians were blinded to limb exposure, and the loaded tendon was compared to the matched, non-loaded limb of the same animal. Therefore, there may be disruptions in tissue architecture caused by the histology preparation method, but the differences observed between limbs are due to the effects of loading. In addition, the microtears observed in the control limb may be due to limb loading experienced during normal cage activity. Third, generalizing from the rabbit to the human should be done with caution. In rabbits, the flexor muscles (FDP and FDS) originate at the medial epicondyle but in humans, the FDS originates at the medial epicondyle while the FDP originates along the proximal ulna close to the medial epicondyle. However, the tendon biochemical composition, healing processes, and mechanical properties of rabbit tendon are similar to human [3,4,9,16,26].

The pathophysiology of tendinopathy due to overuse likely involves an accumulation of microstructural damage, generated by mechanical fiber failure and biological mediators, combined with the tendon's inability to repair the damage. One possible degenerative pathway may involve microtear formation that may induce tendon cells to release matrix metalloproteinases or cytokines, which may further degrade the tendon's matrix either directly or indirectly by initiating a degradation pathway that may lead to the formation of additional microtears.

This in vivo animal model demonstrates that all three measures of microtears, tear area as a percent of tendon area, tear density, and mean tear size, are increased in tendons cyclically loaded at physiological loads for 80 cumulative hours. In addition, microtear density and size are greater along the outer regions of both loaded and unloaded tendon. Regions with large microtears or increased density of tears are likely to be the nexus of tendinosis and may ultimately undergo the changes typical of epicondylosis such as degenerative changes with new capillary formation and fibrillation.

Acknowledgement

References

[1] Allander E. Prevalence, incidence, and remission rates of some common rheumatic diseases or syndromes. Scand J Rheumatol 1974;3:145–53.

[2] Almekinders LC, Banes AJ, Ballenger CA. Effects of repetitive motion on human fibroblasts. Med Sci Sports Exerc 1993;25:603–7.

[3] Archambault JM, Hart DA, Herzog W. Response of rabbit Achilles tendon to chronic repetitive loading. Connect Tissue Res 2001;42:13–23.

[4] Backman C, Boquist L, Friden J, Lorentzon R, Toolanen G. Chronic achilles paratenonitis with tendinosis: an experimental model in the rabbit. J Orthop Res 1990;8:541–7.

[5] Barbe MF, Barr AE, Gorzelany I, Amin M, Gaughan JP, Safadi FF. Chronic repetitive reaching and grasping results in decreased motor performance and widespread tissue responses in a rat model of MSD. J Orthop Res 2003;21:167–76.

[6] Chard MD, Cawston TE, Riley GP, Gresham GA, Hazleman BL. Rotator cuff degeneration and lateral epicondylitis: a comparative histological study. Ann Rheum Dis 1994;53:30–4.

[7] Chard MD, Hazleman BL. Tennis elbow—a reappraisal. Br J Rheumatol 1989;28:186–90.

[8] Cvitanic O, Henzie G, Skezas N, Lyons J, Minter J. MRI diagnosis of tears of the hip abductor tendons (gluteus medius and gluteus minimus). AJR Am J Roentgenol 2004;182:137–43.

[9] Enwemeka CS. Inflammation, cellularity, and fibrillogenesis in regenerating tendon: implications for tendon rehabilitation. Phys Ther 1989;69:816–25.

[10] Gibbon WW, Cooper JR, Radcliffe GS. Sonographic incidence of tendon microtears in athletes with chronic Achilles tendinosis. Br J Sports Med 1999;33:129–30.

[11] Jozsa L, Kannus P. Histopathological findings in spontaneous tendon ruptures. Scand J Med Sci Sports 1997;7:113–8.

[12] Kannus P. Tendons—a source of major concern in competitive and recreational athletes. Scand J Med Sci Sports 1997;7:53–4.

[13] Kraushaar BS, Nirschl RP. Tendinosis of the elbow (tennis elbow). Clinical features and findings of histological, immunohistochemical, and electron microscopy studies. J Bone Joint Surg Am 1999;81:259–78.

[14] La S, Fessell DP, Femino JE, Jacobson JA, Jamadar D, Hayes C. Sonography of partial-thickness quadriceps tendon tears with surgical correlation. J Ultrasound Med 2003;22:1323–9. quiz 1330–1.

[15] Maffulli N, Khan KM, Puddu G. Overuse tendon conditions: time to change a confusing terminology. Arthroscopy 1998;14:840–3.

[16] Malaviya P, Butler DL, Boivin GP, Smith FN, Barry FP, Murphy JM, et al. An in vivo model for load-modulated remodeling in the rabbit flexor tendon. J Orthop Res 2000;18:116–25.

[17] Messner K, Wei Y, Andersson B, Gillquist J, Rasanen T. Rat model of Achilles tendon disorder. A pilot study. Cells Tissues Organs 1999;165:30–9.

[18] National Research Council (U.S.), 2001. Panel on Musculoskeletal Disorders and the Workplace, Institute of Medicine (U.S.): Musculoskeletal disorders and the workplace: low back and upper extremities, p. xv, 492. Washington, DC, National Academy Press.

[19] Ohashi K, El-Khoury GY, Bennett DL. MDCT of tendon abnormalities using volume-rendered images. AJR Am J Roentgenol 2004;182:161–5.

[20] Pfahler M, Jessel C, Steinborn M, Refior HJ. Magnetic resonance imaging in lateral epicondylitis of the elbow. Arch Orthop Trauma Surg 1998;118:121–5.

[21] Potter HG, Hannafin JA, Morwessel RM, DiCarlo EF, O'Brien SJ, Altchek DW. Lateral epicondylitis: correlation of MR

imaging, surgical, and histopathologic findings. Radiology 1995;196:43–6.

[22] Regan W, Wold LE, Coonrad R, Morrey BF. Microscopic histopathology of chronic refractory lateral epicondylitis. Am J Sports Med 1992;20:746–9.

[23] Soslowsky LJ, Thomopoulos S, Esmail A, Flanagan CL, Iannotti JP, Williamson 3rd JD, et al. Rotator cuff tendinosis in an animal model: role of extrinsic and overuse factors. Ann Biomed Eng 2002;30:1057–63.

[24] Soslowsky LJ, Thomopoulos S, Tun S, Flanagan CL, Keefer CC, Mastaw J, et al. Neer Award 1999. Overuse activity injures the supraspinatus tendon in an animal model: a histologic and biomechanical study. J Shoulder Elbow Surg 2000;9:79–84.

[25] Steinborn M, Heuck A, Jessel C, Bonel H, Reiser M. Magnetic resonance imaging of lateral epicondylitis of the elbow with a 0.2-T dedicated system. Eur Radiol 1999;9:1376–80.

[26] Stone D, Green C, Rao U, Aizawa H, Yamaji T, Niyibizi C, et al. Cytokine-induced tendinitis: a preliminary study in rabbits. J Orthop Res 1999;17:168–77.

[27] Tallon C, Maffulli N, Ewen SW. Ruptured Achilles tendons are significantly more degenerated than tendinopathic tendons. Med Sci Sports Exerc 2001;33:1983–90.

[28] Tsuzaki M, Guyton G, Garrett W, Archambault JM, Herzog W, Almekinders L, et al. IL-1 beta induces COX2, MMP-1, -3 and -13, ADAMTS-4, IL-1 beta and IL-6 in human tendon cells. J Orthop Res 2003;21:256–64.

[29] United States. Bureau of Labor Statistics: Occupational injuries and illnesses–counts, rates, and characteristics, p. v. Washington, DC, The Bureau: For sale by the US G.P.O. Supt. of Docs, 1995.

[30] Vogel KG. The effect of compressive loading on proteoglycan turnover in cultured fetal tendon. Connect Tissue Res 1996;34:227–37.

[31] Waggett AD, Ralphs JR, Kwan AP, Woodnutt D, Benjamin M. Characterization of collagens and proteoglycans at the insertion of the human Achilles tendon. Matrix Biol 1998;16:457–70.

[32] Wakabayashi I, Itoi E, Sano H, Shibuya Y, Sashi R, Minagawa H, et al. Mechanical environment of the supraspinatus tendon: a two-dimensional finite element model analysis. J Shoulder Elbow Surg 2003;12:612–7.

[33] Wetzel BJ, Nindl G, Swez JA, Johnson MT. Quantitative characterization of rat tendinitis to evaluate the efficacy of therapeutic interventions. Biomed Sci Instrum 2002;38:157–62.

[34] Yu JS, Popp JE, Kaeding CC, Lucas J. Correlation of MR imaging and pathologic findings in athletes undergoing surgery for chronic patellar tendinitis. AJR Am J Roentgenol 1995;165:115–8.